Histamine and its contributory role in promoting organ injury in sepsis

敗血症による臓器傷害進展におけるヒスタミンの寄与

2016

Mizuki Hattori

Department of Anesthesiology, Graduate School of Medicine and Pharmaceutical Sciences, University of Toyama, Toyama, Japan

Table of Contents

INTRODUCTION

Sepsis is a common and potentially life-threatening medical condition in populations in intensive care units. Despite advances in overall care of critically ill patients, sepsis remains the primary cause of death from microbial infections (1, 2). The development of a failure of one or more organs, including lung, kidney, and liver, poses a major threat to the survival of patients with sepsis. In accordance with the importance of more timely management of patients with sepsis or at risk of developing sepsis, sepsis is now defined as life-threatening organ dysfunction due to a dysregulated host response to infection (3). The pathogenesis of sepsis-induced organ failure has been extensively gleaned from animal models and human studies (4-6), but the mechanisms underlying the pathophysiologic processes that both initiate and promulgate organ dysfunction in sepsis have not been fully elucidated. A greater understanding of the mechanisms that underlie the development of organ dysfunction in sepsis may enable us to develop therapies targeted at preventing or limiting molecular events associated with the progress of fatal organ failure, and hence leading to improve outcomes.

In animal models and in septic patients, elevated plasma levels of histamine have been documented for a long time (7). In our previous studies, the sustained elevation of plasma histamine has been shown to be associated with the time-dependent increase in expression of histidine decarboxylase (HDC), which is the catabolic enzyme of histamine synthesis, in the animals with lipopolysaccharide (LPS)- and cecal ligation and puncture (CLP)-induced sepsis (8-10). Furthermore, endotoxemia may cause superinduction of H_1- and H_2-receptors in cardiovascular and pulmonary tissues (8, 9, 11). Since histamine mediates a wide range of cellular responses, including allergic and inflammatory reactions, gastric acid secretion, vascular tone and permeability, and neurotransmission in the central

nervous system (12), the histamine biological responsiveness may be of special importance in certain pathological aspects suggestive of histamine release. It would be thus allowable to assume that histamine may play a contributory role in the development of major organ dysfunction and failure associated with sepsis.

In the present study, we examined whether genetic and pharmacological interventions of histamine can provide a change in systemic inflammation and organ injury in mice with CLP-induced polymicrobial sepsis in order to explore the role of histamine in the pathophysiology of the septic syndrome. CLP-induced sepsis is an animal model that has high relevance to humans because it reproduces many hallmarks of sepsis that occur in patients (13). We applied HDC gene knockout ($HDC^{-/-}$) mice (14), lacking histamine, to investigate the effect of histamine deficiency on the pathophysiology of CLP-induced sepsis. Along with $HDC^{-/-}$ mice, we also used histamine H_1-/H_2-receptor gene-double knockout ($H_1R^{-/-}/H_2R^{-/-}$) mice generated by crossbreeding of H_1-receptor null mice and H_2-receptor null mice. Finally, we tested changes in the pathophysiological features of CLP-induced sepsis by pharmacological antagonism of H_1- and H_2-receptors.

MATERIALS AND METHODS

Generation of $HDC^{-/-}$ mice and $H_1R^{-/-}/H_2R^{-/-}$ mice

$HDC^{-/-}$ mice were generated according to previously described procedures (14). H_1-receptor gene deficient mice and H_2-receptor gene deficient mice were a gift from Prof. Kazuhiko Yanai, Tohoku University (15, 16), and the progeny of the colony was maintained. Serially breeding of these two strains generated the double-knockout line ($H_1R^{-/-}/H_2R^{-/-}$). Genotyping of the resultant mice was determined by PCR analysis of DNA extracted from tail samples. $HDC^{-/-}$ mice and $H1R^{-/-}/H2R^{-/-}$ mice were of a genetic background of a C57BL/6J strain, and their littermates were used as wild-type (WT) controls. Mice were housed under specific-pathogen-free conditions.

Animal model of sepsis

All animal studies were conducted in accordance with the National Institute of Health Guidelines on the use of laboratory animal and with approval of the Care and Use Committee of the University of Toyama. The surgical procedure to generate CLP-induced sepsis was performed as described elsewhere (17-19). In brief, male mice, 8-10 weeks old, were anesthetized with 3-4% sevoflurane, and a middle abdominal incision was made. The cecum was mobilized, ligated, and punctured twice with a 21-gauge needle, allowing exposure of faces, the bowel was repositioned, and the abdomen was closed with sterile suture. Sham-operated control underwent the same procedure except for ligation and puncture of the cecum. A noninvasive computerized tail-cuff system was used for measuring blood pressure and heart rate in mice (17, 20).

Measurement of histamine

The amount of histamine was determined by the fluorometrical method with *o*-phthalaldehyde (21). The tissues were homogenized in 4-5 volumes of PBS containing 2 M NaCl, lysed using 0.5% Triton X-100, and centrifuged at 12,000 × *g* for 30 min at 4ºC in order to obtain the soluble fraction for histamine assay.

RNA extraction and quantitative real-time PCR

Total RNA was isolated from tissues with Sepazol-RNA I Super G (Nacalai Tesque, Kyoto, Japan). PrimeScript RT Master Mix (Takara Bio, Ohtsu, Japan) or ReverTra Ace qPCR RT Master Mix (Toyobo, Osaka, Japan) was used for the reverse transcription reaction, and real-time PCR analyses were performed using SYBR Premix Ex Taq II (Takara Bio). Glyceraldehyde-3-phosphate dehydrogenase (GAPDH) was used as the endogenous control, and fold increase was calculated according to $\Delta\Delta C_T$ method.

Serum analyzes

Blood was collected in serum gel tubes (Sarsted, Nümbrecht, Germany), and serum was obtained and stored at -80ºC. The quantitative determination of aspartate aminotransferase (AST), alanine aminotransferase (ALT), blood urea nitrogen (BUN), and creatinine in serum was made on Hitachi 7180 Biochemistry Automatic Analyzer (Hitachi High-Technologies, Tokyo, Japan). Interleukin (IL)-1β, IL-6, tumor necrosis factor (TNF)-α, and monocyte chemotactic protein (MCP)-1 were measured by the use of a commercially available enzyme-linked immunosorbent assay (ELISA) kit (R&D Systems, Minneapolis, MN, USA), according to the manufacturer's instructions. The plate was read on a microplate reader (Nippon-InterMed, Tokyo, Japan). Assays were performed in duplicate.

Lung wet-to-dry weight ratio

Surgically removed lung tissues were blotted dry and weighed to determine the lung wet weight. The lung tissues were then wrapped loosely in aluminum foil, placed in a drying oven overnight, and weighed again for calculation of the wet-to-dry weight ratio (9, 22).

Histologic examination

Tissues were fixed by immersion in 10% buffered formaldehyde overnight, embedded in paraffin, and cut into 4-μm-thick sections. After deparaffinization, slides were stained with hematoxylin and eosin by standard methods. All the histological studies were performed in a blinded fashion.

Immunohistochemistry

Tissue sections (4 μm) were rehydrated, and endogenous peroxidases were quenched with 3% hydrogen peroxide. Slides were then incubated overnight at 4°C with primary antibodies for myeloperoxidase (MPO; 1:200 dilution; Abcam, Cambridge, MA, USA), or neutrophil gelatinase-associated lipocalin (NGAL; 1:2000; Abcam). All sections were incubated with Histone® Simple Stain Mouse MAX PO(R) (Nichirei Biosciences, Tokyo, Japan) including the secondary antibody which is reduced to Fab fragment. Sections were developed with 3,3'-diaminobenzidine and counterstained with hematoxylin. Rabbit IgG was used as an isotype control.

Immunofluorescence staining

The tissue sections were exposed to the fluorescent antibody Alexa Fluor 546-conjugated anti-mouse IgG (Invitrogen, Carlsbad, CA, USA) after overnight incubation

with the primary antibody according to the method in our previous study with minor modification (20). The nucleus was counterstained with Hoechst 33342 dye (Invitrogen). Immunofluorescence images were observed under an Olympus (Tokyo, Japan) BX-51 fluorescence microscope and processed using Adobe Photoshop CC software (Adobe, San Jose, CA, USA).

Western blot analysis

After being removed and rinsed in sterilized PBS on ice, tissues were homogenized and then centrifuged at 18,000 × *g* for 10 min at 4°C, and the resulting supernatants were collected. When required, nuclear protein extracts from lungs were obtained with a commercially available nuclear extraction kit (Sigma-Aldrich, St. Louis, MO, USA), as described in the manufacturer's manual. The proteins in the supernatant were measured using BCA Protein Assay Kit (Thermo Fisher Scientific, Rockford, IL, USA). Immunoblotting was performed as described in our previous reports (19, 23). Samples (30-50 μg of protein) were electrophoresed on 10 or 14% SDS-PAGEs and transferred to PVDF membrane. For primary antibody incubation (overnight at 4°C), rabbit polyclonal or monoclonal antibodies were used against NGAL (1:1,000; Abcam), IκBα (1:1,000; Cell Signaling, Danvers, MA, USA), and phospho-IκBα (Ser-32) (1:1,000; Cell Signaling), , whereas a mouse monoclonal antibody was used against nuclear factor (NF)-κB (1:200; Santa Cruz Biotechnology, Santa Cruz, CA, USA), β-actin (1:5,000; Wako Pure Chemical, Osaka, Japan), and GAPDH (1:5,000; Wako Pure Chemical) and a goat polyclonal antibody against lamin B (1:200; Santa Cruz Biotechnology). Primary antibody detection was performed with horseradish peroxidase-conjugated secondary antibodies. Binding of the antibody was detected by an ImmunoStar Zeta (Wako Pure Chemical) and levels of protein expression were quantitated by a luminoimage LAS-4000

analyzer (Fuji Film, Tokyo, Japan).

Statistics

Values are expressed as means ± SEM. Statistical significance between groups was evaluated by ANOVA and the Tukey multiple comparison test using Prism software (ver. 6; GraphPad Software, San Diego, CA, USA). $P \leq 0.05$ was considered statistically significant.

RESULTS

Changes in tissue histamine concentrations, HDC expression, and histamine receptor expression after sepsis induction

We initially ascertained whether tissue histamine synthesis is altered in WT mice after sepsis induction by CLP. As demonstrated in our previous report (10), CLP-induced polymicrobial sepsis resulted in an increase in plasma concentrations of histamine in mice (data not shown). Thus, plasma histamine concentrations were significantly ($P<0.05$) elevated from baseline of 16.1 ± 3.5 ng/mL (n = 4) early after CLP, with a peak concentration at 3 h (38.9 ± 3.5 ng/mL, n = 4). The basal levels of histamine highly varied between tissues (lung, 349 ± 87 ng/g; liver, 7.9 ± 2.7 ng/g; kidney, 165 ± 14 ng/g, n = 13 for each). When sepsis was induced by CLP, however, histamine levels elevated in all tissues in a time-dependent manner (Fig. 1*A*). In mammalian tissues, histamine is synthesized from L-histidine by HDC. Real-time PCR analysis showed that the transcript levels of HDC were transiently but greatly increased in all tissues after induction of sepsis (Fig. 1*B*).

Changes in histamine H_1- and H_2-receptor mRNA expression in lung, liver, and kidney tissues of WT mice after sepsis induction were also examined by real-time PCR (Fig. 1*B*). In lung tissues, no increase in H_1-receptor mRNA expression was observed after CLP. On the other hand, the mRNA levels were increased 3.2-fold and 3.1- to 4.4 fold in liver and kidney tissues, respectively, at 6-12 h after CLP when compared with those shown in controls. Following induction of sepsis by CLP, a significant increase in H_2-receptor mRNA expression was transiently detected in lung and liver tissues. In the kidney, CLP-induced sepsis resulted in a sustained, significant increase in the transcript level of H_2-receptors.

Sepsis-induced inflammation and organ injury are alleviated in HDC knockout mice

When blood levels of proinflammatory or chemotactic cytokines were measured using an ELISA, the sham-operated control animals had low levels of the cytokines examined here and no difference was found between WT and $HDC^{-/-}$ mice (Fig. 2*A*). The animals 18 h after CLP-induced sepsis had marked elevations in IL-1β, IL-6, TNF-α, and MCP-1. Following sepsis induction, however, $HDC^{-/-}$ mice displayed an evidently lower levels of those cytokines compared with WT mice. We also examined changes in mRNA levels of IL-1β, IL-6, TNF-α, and MCP-1 in lung, liver, and kidney tissues using real-time PCR (Fig. 2*B*). After induction of sepsis, mRNA expression levels of those cytokines greatly increased in all tissues. The increases in their mRNA expression showed a trend toward declining in $HDC^{-/-}$ mice, with a few exceptions.

The animals subjected to CLP showed a sharp fall in systolic blood pressure (data not shown). No significant difference in hypotension was observed between WT and $HDC^{-/-}$ mice after CLP. The CLP-induced sepsis caused a transient decrease in the heart rate in both WT and $HDC^{-/-}$ mice, but the heart rate responses of the two animal groups were not substantially different. $HDC^{-/-}$ mice had a survival advantage after CLP as compared with WT controls (data not shown).

Histologic examination of hematoxylin and eosin-stained sections of the lungs showed massive infiltration of inflammatory cells, disorganized architecture with irregular alveoli, and intra-alveolar hemorrhage arising from capillary rupture in WT mice 24 h after sepsis induction by CLP (Fig. 3*A*). In lungs from $HDC^{-/-}$ mice, these histopathological changes were lessened. Semiquantitative assessment using lung injury score revealed that the score was significantly lower in $HDC^{-/-}$ mice than in WT controls. The sepsis-induced increase in lung staining of MPO, an index of neutrophil infiltration, was significantly reduced in $HDC^{-/-}$ mice in comparison with WT controls (Fig. 3*B*). When

the wet-to-dry lung weight ratio was measured for assessment of lung vascular leak, the ratio was significantly increased in WT mice after sepsis induction (Fig. 3*C*). However, the sepsis-induced rise in the ratio in $HDC^{-/-}$ mice was blunted.

Following induction of sepsis by CLP, a marked elevation in serum levels of AST and ALT, a functional readout for liver damage, was observed in WT mice (Fig. 4*A*). The elevation in these serum aminotransferase levels after sepsis was significantly lowered in $HDC^{-/-}$ mice. When liver injury was assessed using liver specimens stained with hematoxylin and eosin, massive alterations in hepatocytes, including irregular contour of cells and nuclei, cytoplasmic vacuolation, cytoplasmic and nuclear degeneration, and cellular rupture, were found in WT mice after sepsis induction (Fig. 4*B*). A destruction of the sinusoidal structure of the liver and erythrocyte agglutination were also observed. Such histopathological alterations showing the liver damage after sepsis was less pronounced in $HDC^{-/-}$ mice. Furthermore, the highly increased neutrophilic influx in the liver from septic WT mice was indicated by MPO staining (Fig. 4*C*). There was much lower MPO expression in liver specimens from $HDC^{-/-}$ mice.

The serum levels of BUN and creatinine, both of which provide a guide to kidney function, were markedly elevated in septic WT mice (Fig. 5*A* and *B*). Pathologically elevated serum BUN and creatinine levels were reduced in $HDC^{-/-}$ mice. No apparent histopathological finding was detectable even in WT mice after sepsis induction when the renal tissue sections were stained using hematoxylin and eosin (Fig. 5*C*). However, we found that septic WT mice displayed the intense staining of NGAL, a biomarker of kidney damage (Fig. 5*D*). $HDC^{-/-}$ mice following sepsis induction exhibited weaker NGAL staining in kidneys. In line with the findings from immunohistochemical assessment of renal NGAL, Western blot analysis showed that a striking rise in renal expression of NGAL caused by sepsis was more evident in WT as compared with $HDC^{-/-}$ mice (Fig. 5*E*).

Sepsis-induced NF-κB activation is reduced in HDC knockout mice

We examined whether sepsis-induced activation of the transcription factor NF-κB is altered in $HDC^{-/-}$ mice. Since the activity of NF-κB is primarily regulated by interaction with its inhibitory protein IκBα, phosphorylation and degradation of IκBα in lung tissues after sepsis induction were monitored by Western blot (Fig. 6*A*). Induction of sepsis resulted in greatly increased phosphorylation and degradation of IκBα in lungs of WT mice. Such changes were diminished in $HDC^{-/-}$ mice. The translocation of NF-κB p65 into the nucleus was increased in lung nuclear extracts from septic WT mice (Fig. 6*B*). In $HDC^{-/-}$ mice, the nuclear translocation of NF-κB p65 was weak. In line with this finding, nuclear staining for NF-κB 65 was more detectable in WT than in $HDC^{-/-}$ mice after sepsis induction (Fig. 6*C*).

Effects of H_1- and H_2-receptor antagonists on sepsis-induced inflammation and organ injury

Mice were injected intraperitoneally with a single dose of *d*-chlorpheniramine (10 mg/kg) and famotidine (20 mg/kg) 60 min before CLP to block H_1- and H_2-receptors, respectively. The elevated blood levels of pro-inflammatory and chemotactic cytokines after sepsis appeared to be reduced more by combined treatment with *d*-chlorpheniramine and famotidine than with each blocker alone, although their treatment alone was effective in reducing some cytokines (such as TNF-α) in blood (Fig. 7*A*). Furthermore, the sepsis-induced increases in tissue levels of IL-1β, IL-6, and TNF-α mRNAs were lowered when the two blockers were given together to the animals (data not shown).

When CLP-induced septic mice received treatment with *d*-chlorpheniramine, famotidine, or both, the histological damage in the lung was apparently minimized, as characterized by less distortion of alveolar architecture, scattered interstitial infiltrates, and

rare areas of focal hemorrhage (Fig. 7*B*). Moreover, the sepsis-induced increase in MPO-positive cells was blunted by each treatment (Fig. 7*B*). In liver histology, *d*-chlorpheniramine, famotidine, or both showed a protective effect on liver damage caused by CLP-induced sepsis (Fig. 7*B*). The serum ALT levels were markedly increased from 44 ± 15 (n = 7) to 266 ± 20 IU/L (n = 13, P<0.001) at 18 h after sepsis induction, which was reduced to 159 ± 27 (n = 9, P<0.01) and 136 ± 15 (n = 10, P<0.001) by treatment with *d*-chlorpheniramine and famotidine, respectively. In the kidney, intense accumulation of immunoreactive NGAL that came along with sepsis remained unchanged with *d*-chlorpheniramine, but was attenuated by famotidine alone or combined with *d*-chlorpheniramine (Fig. 7*B*). Consistent with this finding, serum BUN and creatinine levels showed no difference between septic mice untreated and treated with *d*-chlorpheniramine (77 ± 8 *vs*. 84 ± 20 mg/dL and 0.37 ± 0.12 *vs*. 159 ± 27 mg/dL, n = 9-13), but famotidine treatment significantly lowered the rise in the serum markers (54 ± 13 mg/dL and 0.18 ± 0.02 mg/dL, n = 10).

CLP-induced sepsis in H_1-/H_2-receptor double knockout mice

When $H1R^{-/-}/H2R^{-/-}$ mice were rendered septic by CLP, the rise in blood levels of cytokines, IL-6 and MCP-1, was evidently attenuated (Fig. 8*A*). In addition, $H1R^{-/-}/H2R^{-/-}$ mice exhibited lower levels of IL-1β, IL-6, and MCP-1 mRNAs in lung, liver, and kidney tissues as compared with WT mice following sepsis (Fig. 8*B*). When serum ALT in $H1R^{-/-}/H2R^{-/-}$ mice was measured as a marker indicative of liver damage, the markedly increased level following induction of sepsis was subsided (Fig. 8*C*). Also, the high levels of serum BUN and creatinine, routine measures of kidney function, observed after sepsis induction were alleviated in $H1R^{-/-}/H2R^{-/-}$ mice (Fig. 8*D*).

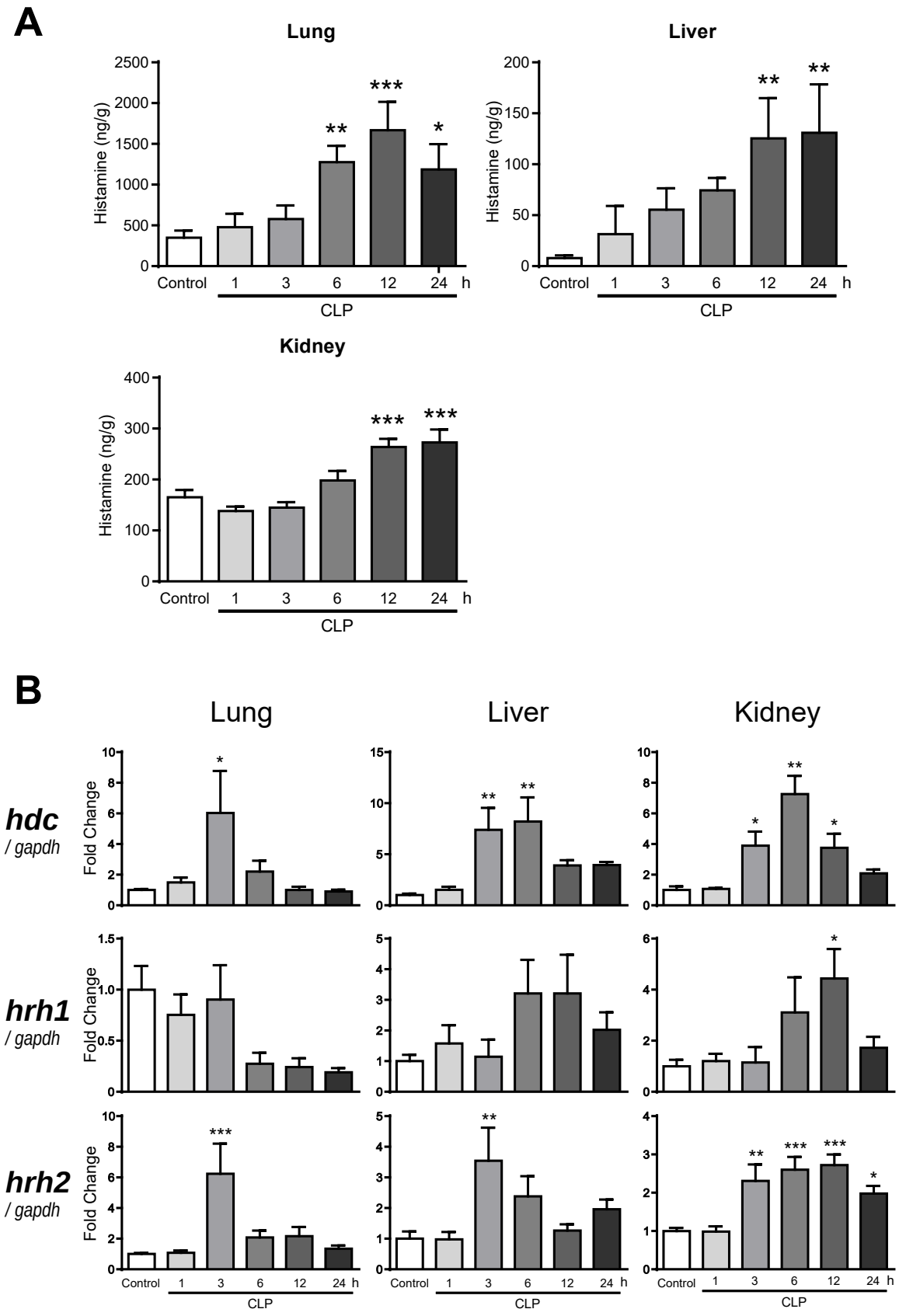
A
Lung
Liver
Kidney
Histamine (ng/g)
Control
1
3
6
12
24
h
CLP
B
Lung
Liver
Kidney
hdc
/ gapdh
hrh1
/ gapdh
hrh2
/ gapdh
Fold Change

Figure 1. Changes in histamine synthesis and histamine receptor expression in lung, liver, and kidney tissues from mice after CLP-induced sepsis. *A*) Tissue histamine concentrations after CLP (n = 8/group). *B*) Tissue mRNA levels of HDC, histamine H_1- and H_2- receptors after CLP (n = 6/group). The mRNA levels were quantified by real-time PCR. The values were expressed as a fold increase above control normalized GAPDH. All values are provided as means ± SEM. *P<0.05, **P<0.01, and ***P<0.001 *vs*. control.

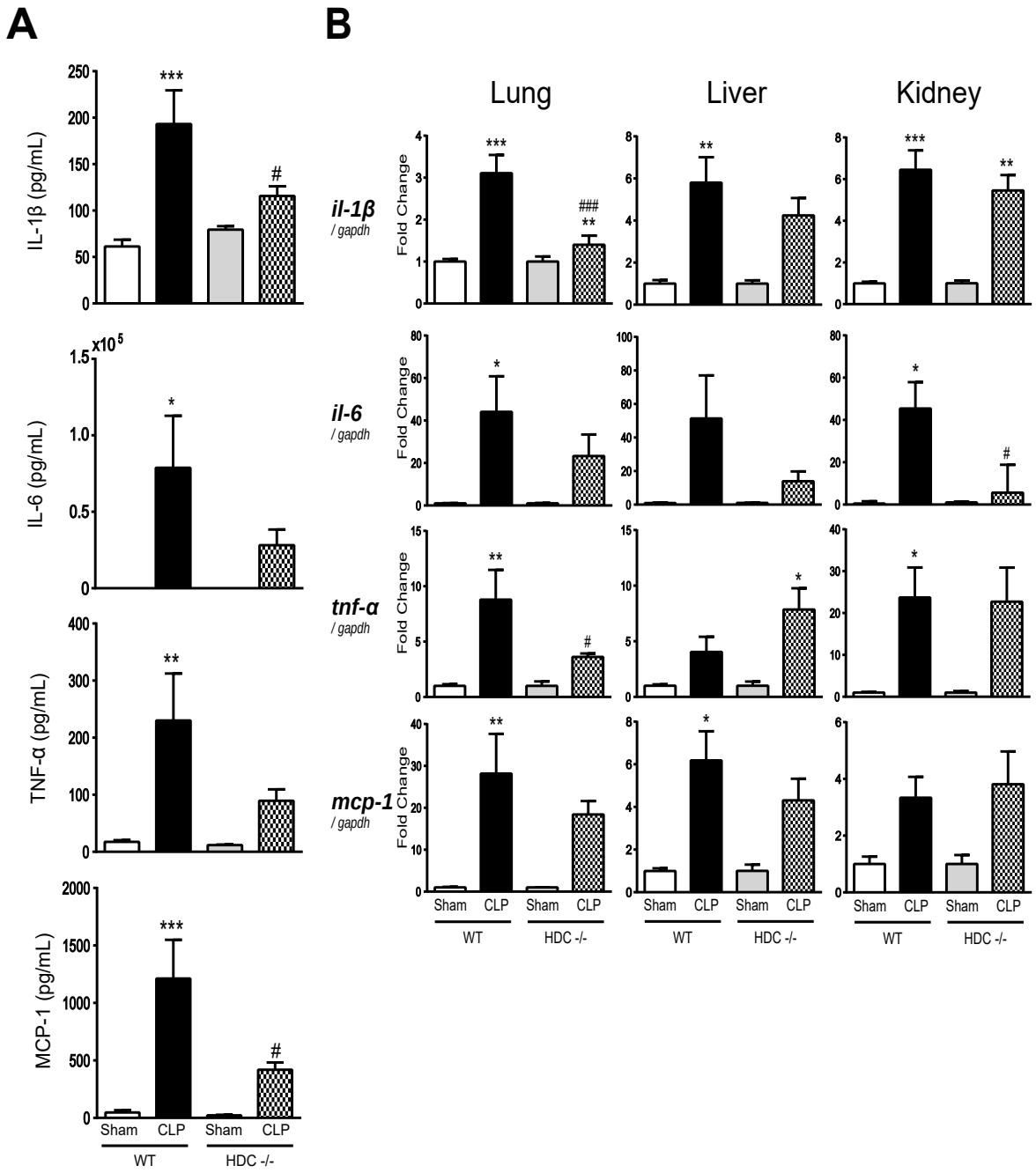
A
B
IL-1β (pg/mL)
IL-6 (pg/mL)
TNF-α (pg/mL)
MCP-1 (pg/mL)
Sham
CLP
WT
HDC -/-
Lung
Liver
Kidney
il-1β
/ gapdh
il-6
/ gapdh
tnf-α
/ gapdh
mcp-1
/ gapdh
Fold Change

Figure 2. Reduced cytokine levels in HDC$^{-/-}$ mice following CLP-induced sepsis. *A*) Blood levels of IL-1β, IL-6, TNF-α, and MCP-1. The blood was collected 18 h after surgery (n = 4-9/group), and those cytokine levels were measured by the use of ELISA. *B*) Transcription levels of IL-1β, IL-6, TNF-α, and MCP-1 in lung, liver, and kidney tissues. Tissues were harvested 18 h after surgery (n = 4-11/group). The mRNA levels were quantified by real-time PCR. The values were expressed as a fold increase above sham-operated control normalized GAPDH. All values are provided as means ± SEM. *P<0.05, **P<0.01, and ***P<0.001 *vs*. the respective control (18 h after sham operation). $^{\#}P$<0.05 *vs*. CLP WT.

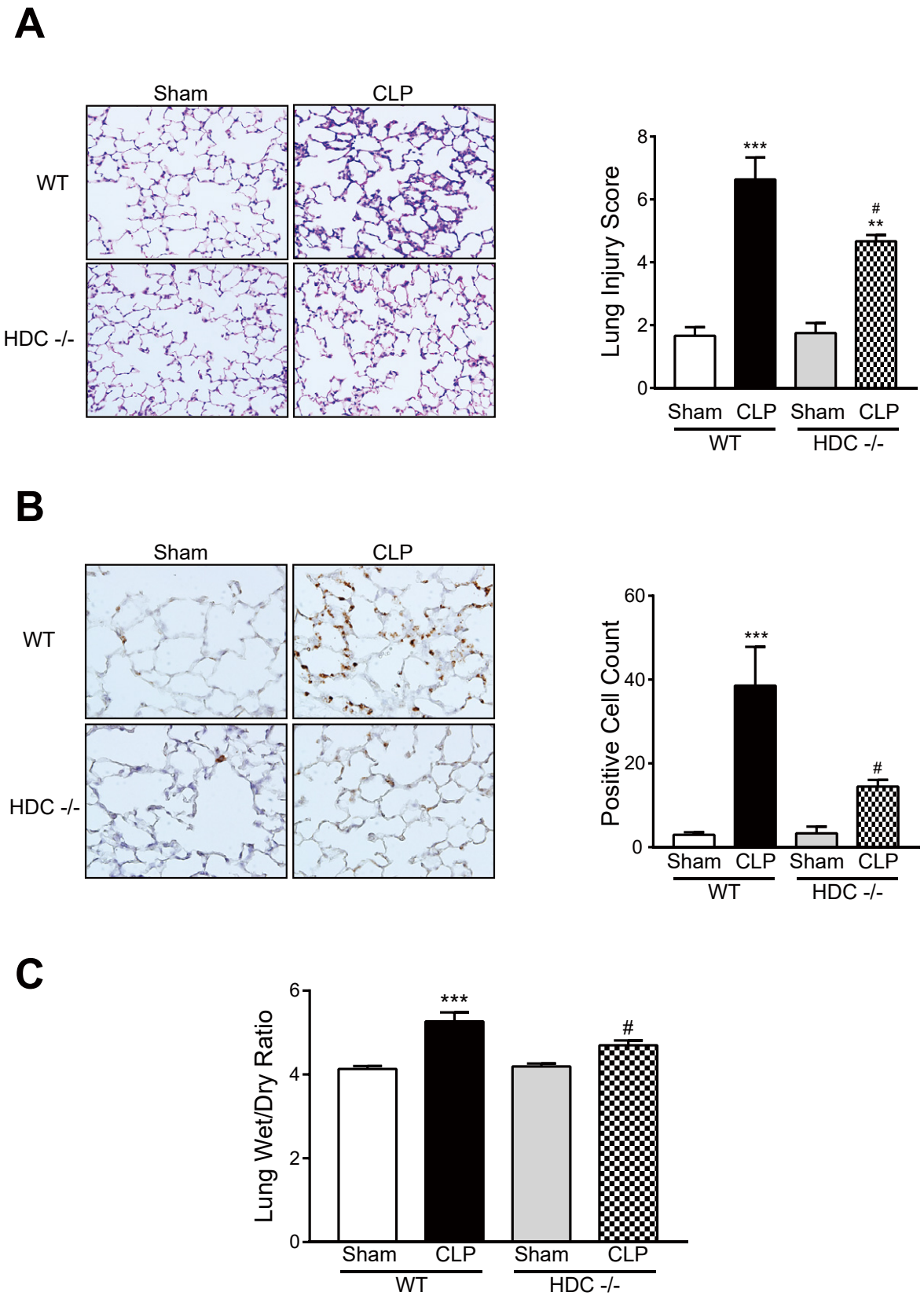
A
Sham
CLP
WT
HDC -/-
Lung Injury Score
***
#
**
Sham
CLP
Sham
CLP
WT
HDC -/-
B
Sham
CLP
WT
HDC -/-
Positive Cell Count
***
#
Sham
CLP
Sham
CLP
WT
HDC -/-
C
Lung Wet/Dry Ratio
***
#
Sham
CLP
Sham
CLP
WT
HDC -/-

Figure 3. Reduced lung injury in $HDC^{-/-}$ mice following CLP-induced sepsis. Lung tissues were harvested from sham-operated and CLP-induced septic mice 24 h after surgery. *A*) Lung sections stained with hematoxylin and eosin. Original magnification, 200×. A bar graph shows semiquantitative analysis of lung tissues by lung injury score, which was performed by scoring from 0-4 (none, light, moderate, severe, and very severe) for the following categories: neutrophil infiltration, pulmonary edema, and disorganization of lung parenchyma and hemorrhage. A total lung injury score was calculated by adding the individual scores in every animal and averaging the total values in each group (n = 4-10/group). *B*) Sections were stained with antibodies against MPO followed by peroxidase staining. Original magnification, 200×. A bar graph shows the summary of quantitation of MPO-positive cell counts. The average of MOP-positive cell number in three fields per sample was calculated (n = 4-10/group). *C*) Wet-to-day ratios of lungs harvested from the animals were determined to assess pulmonary edema (n = 6/group). The summarized results are presented as means ± SEM. $^{*}P<0.05$, $^{**}P<0.01$, and $^{***}P<0.001$ *vs*. the respective control (24 h after sham operation). $^{\#\#}P<0.01$ *vs*. CLP WT.

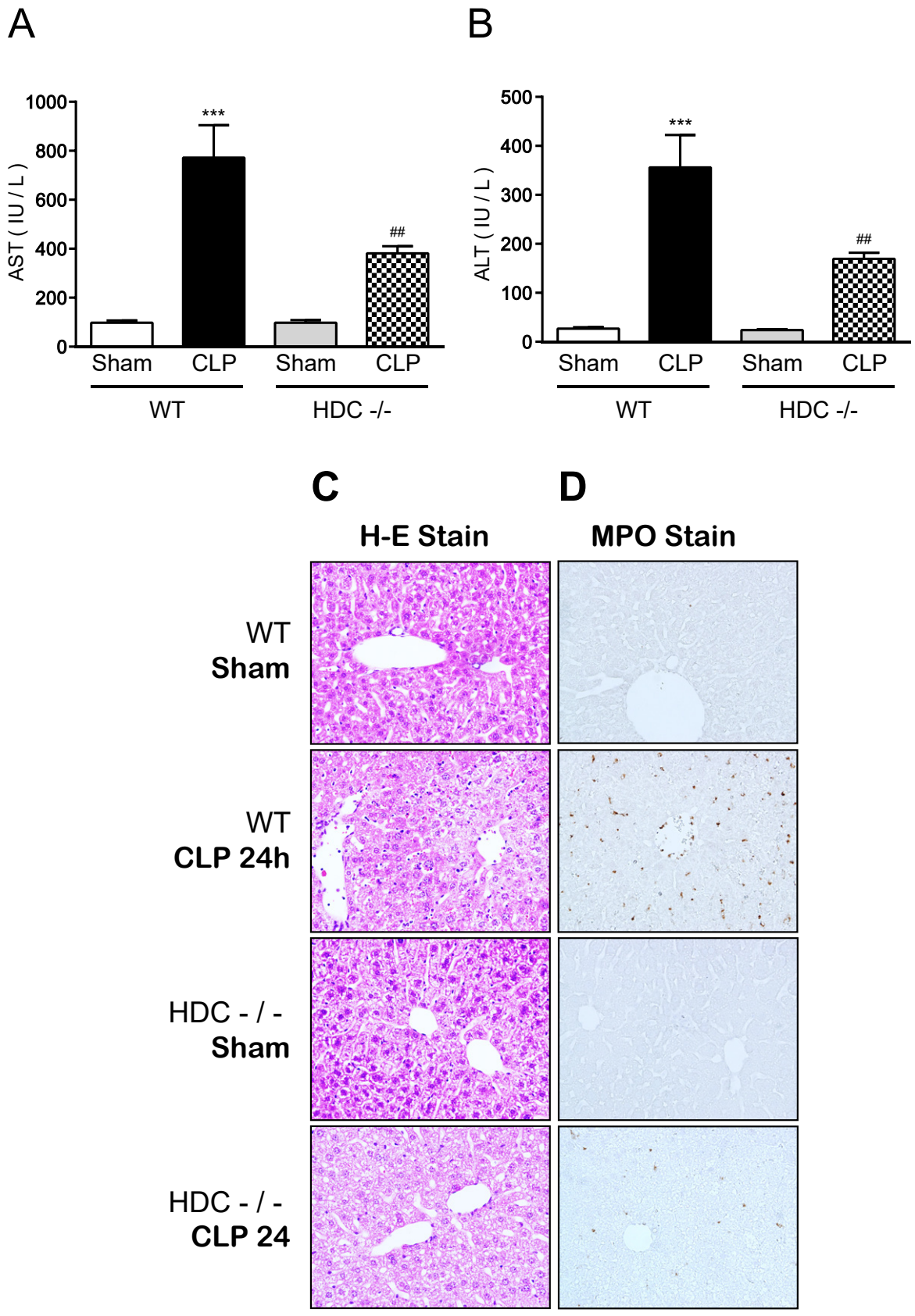
A
B
AST (IU / L)
ALT (IU / L)
1000
800
600
400
200
0
500
400
300
200
100
0
***
##
Sham
CLP
Sham
CLP
WT
HDC -/-
C
D
H-E Stain
MPO Stain
WT
Sham
WT
CLP 24h
HDC - / -
Sham
HDC - / -
CLP 24

Figure 4. Reduced liver injury in $HDC^{-/-}$ mice following CLP-induced sepsis. *A, B*) Serum levels of AST and ALT. Blood samples were collected from sham-operated and CLP-induced septic mice 18 h after surgery (n = 4-11/group). All values are provided as means ± SEM. ***P<0.001 *vs*. the respective control (18 h after sham operation). $^{\#\#}P$<0.01 vs. CLP WT. *C, D*) Representative micrographs liver sections stained with hematoxylin and eosin and anti-MPO antibody followed by peroxidase staining. Original magnification, 200×. Tissues were harvested from sham-operated and CLP-induced septic mice 24 h after surgery. The same results were obtained with two other experiments.

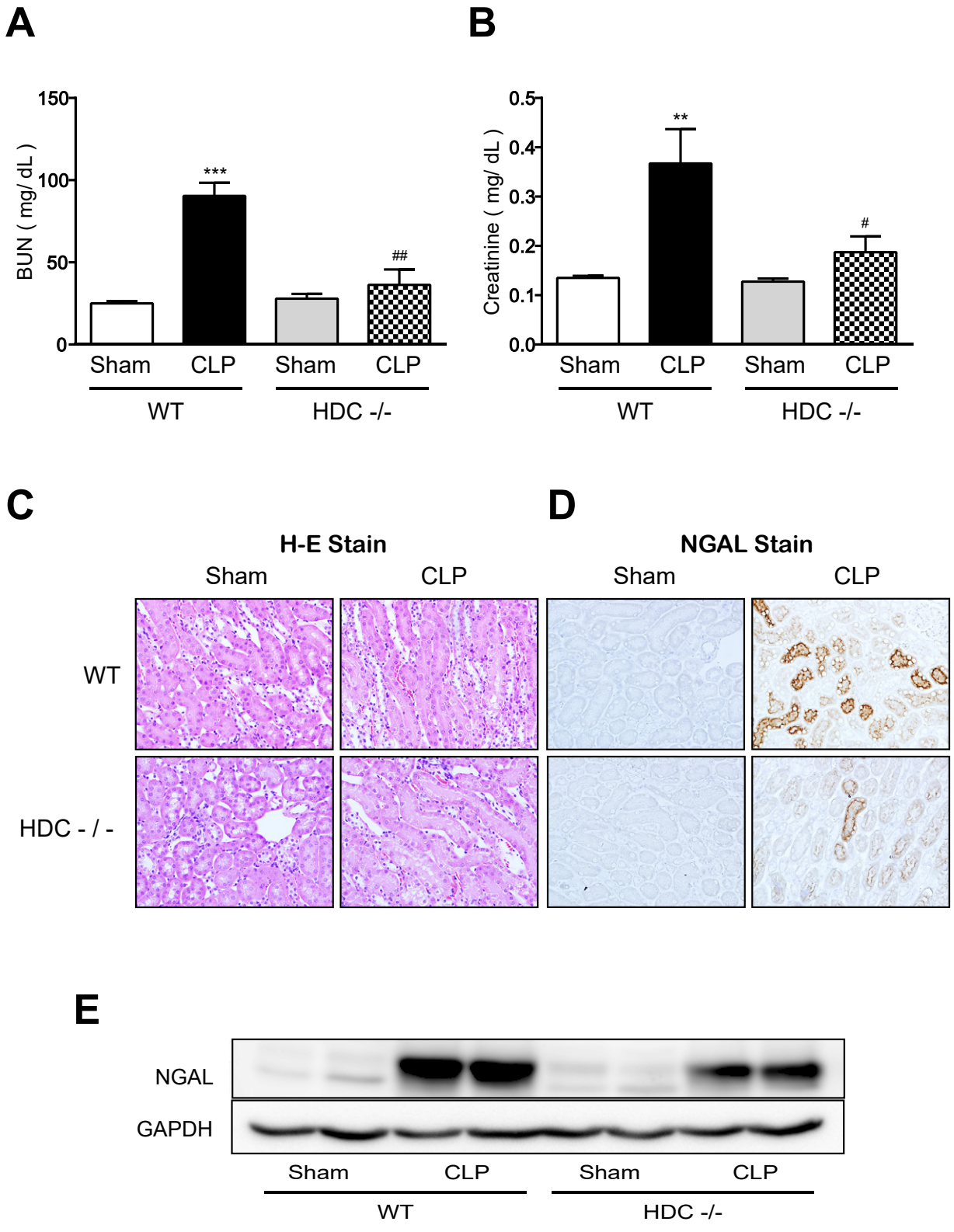
A
B
BUN (mg/ dL)
150
100
50
0
***
##
Sham
CLP
Sham
CLP
WT
HDC -/-
Creatinine (mg/ dL)
0.5
0.4
0.3
0.2
0.1
0.0
**
#
Sham
CLP
Sham
CLP
WT
HDC -/-
C
D
H-E Stain
NGAL Stain
Sham
CLP
Sham
CLP
WT
HDC - / -
E
NGAL
GAPDH
Sham
CLP
Sham
CLP
WT
HDC -/-

Figure 5. Reduced kidney injury in $HDC^{-/-}$ mice following CLP-induced sepsis. *A, B*) Serum levels of BUN and creatinine. Blood samples were collected from sham-operated and CLP-induced septic mice 18 h after surgery (n = 4-11/group). All values are provided as means ± SEM. ***P<0.001 *vs*. the respective control (18 h after sham operation). $^{\#}P$<0.05 and $^{\#\#}P$<0.01 vs. CLP WT. *C, D*) Representative micrographs liver sections stained with hematoxylin and eosin and anti-NGAL antibody followed by peroxidase staining. Original magnification, 200×. The same results were obtained with two other experiments. *E*) Western blot image of NGAL protein expression. GAPDH served as loading control. Shown are representative blots from three independent experiments in which the same results were obtained. Tissues were harvested from sham-operated and CLP-induced septic mice 24 h after surgery.

A

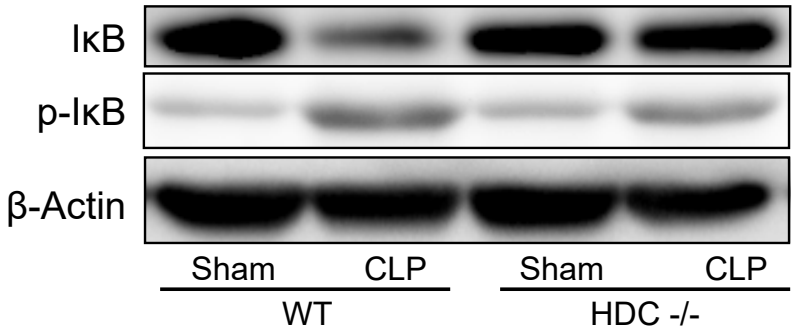
Lung IκB
IκB
p-IκB
β-Actin
Sham
CLP
Sham
CLP
WT
HDC -/-

B

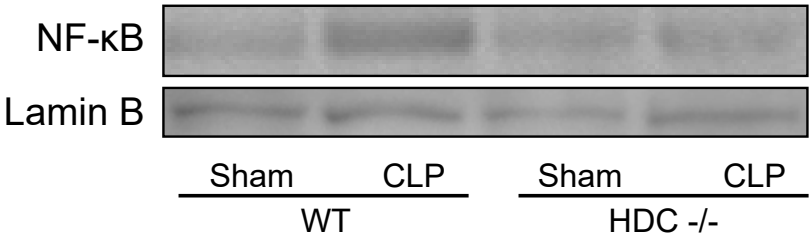
Lung NF-κB
NF-κB
Lamin B
Sham
CLP
Sham
CLP
WT
HDC -/-

C

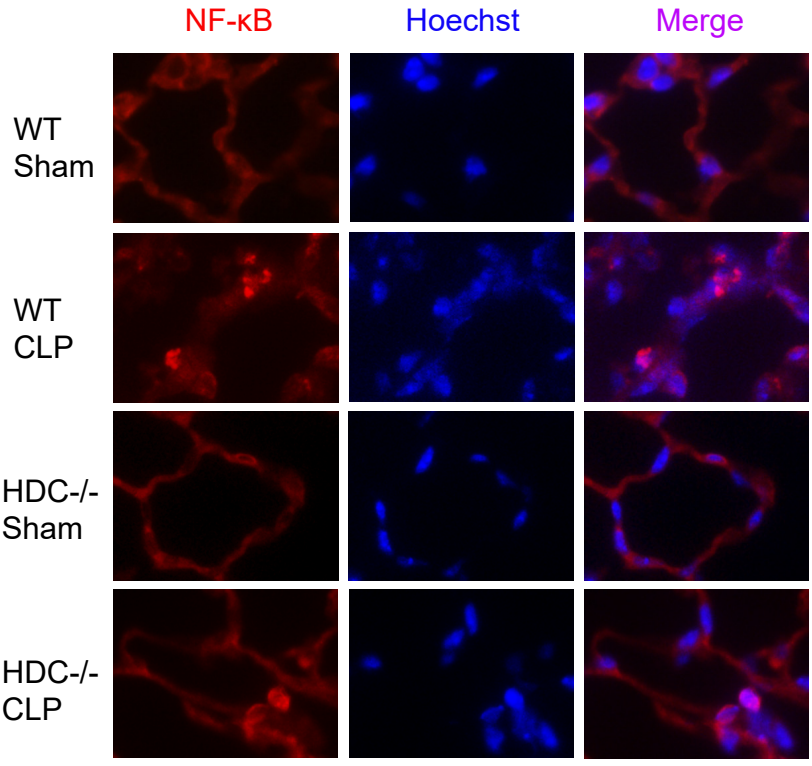
NF-κB
Hoechst
Merge
WT
Sham
WT
CLP
HDC-/-
Sham
HDC-/-
CLP

Figure 6. Kinetics of NF-κB activation in lungs of $HDC^{-/-}$ mice following CLP-induced sepsis. Lung tissues were harvested from sham-operated and CLP-induced septic mice 18 h after surgery. *A*) Western blot analysis using anti-IκBα antibody and anti-phospho-IκBα antibody. β-Actin served as loading control. *B*) Nuclear proteins were extracted, and then NF-κB p65 was detected by Western blot analysis. Lamin B served as a nuclear marker. *C*) Immunofluorescent images for NF-κB p65 (*red*) in lung sections. Nuclei were counterstained with Hoechst 33342 dye (*blue*). Shown are representative blots from two independent experiments in which the same results were obtained.

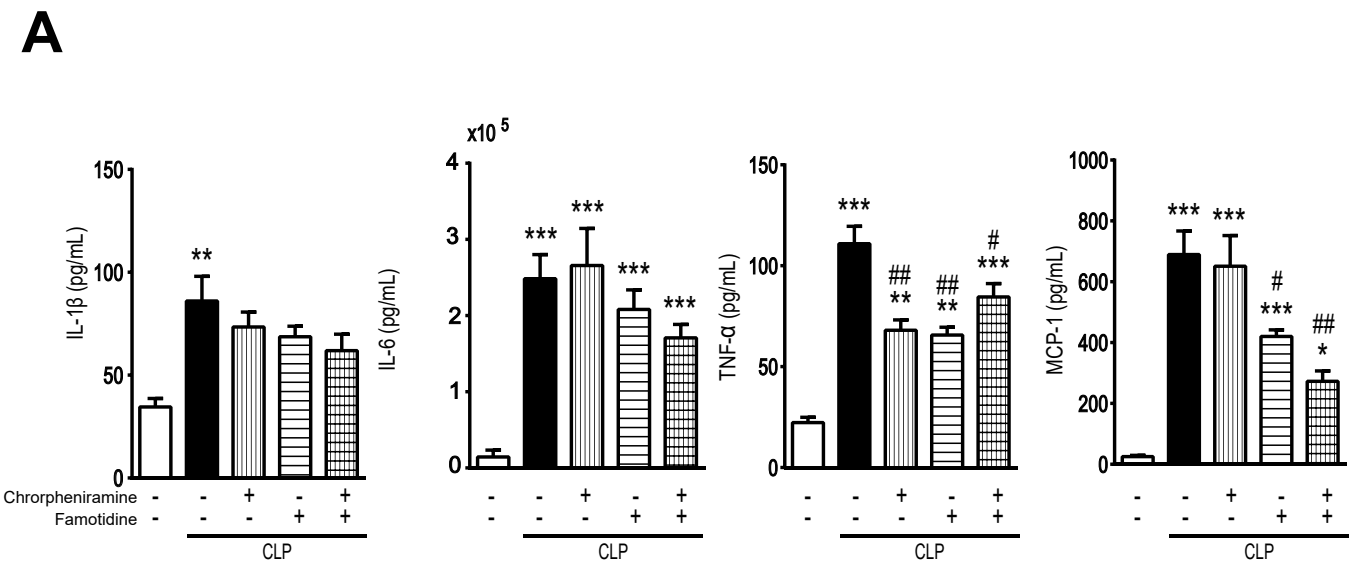
A
IL-1β (pg/mL)
IL-6 (pg/mL)
x10 5
TNF-α (pg/mL)
MCP-1 (pg/mL)
Chrorpheniramine
Famotidine
CLP

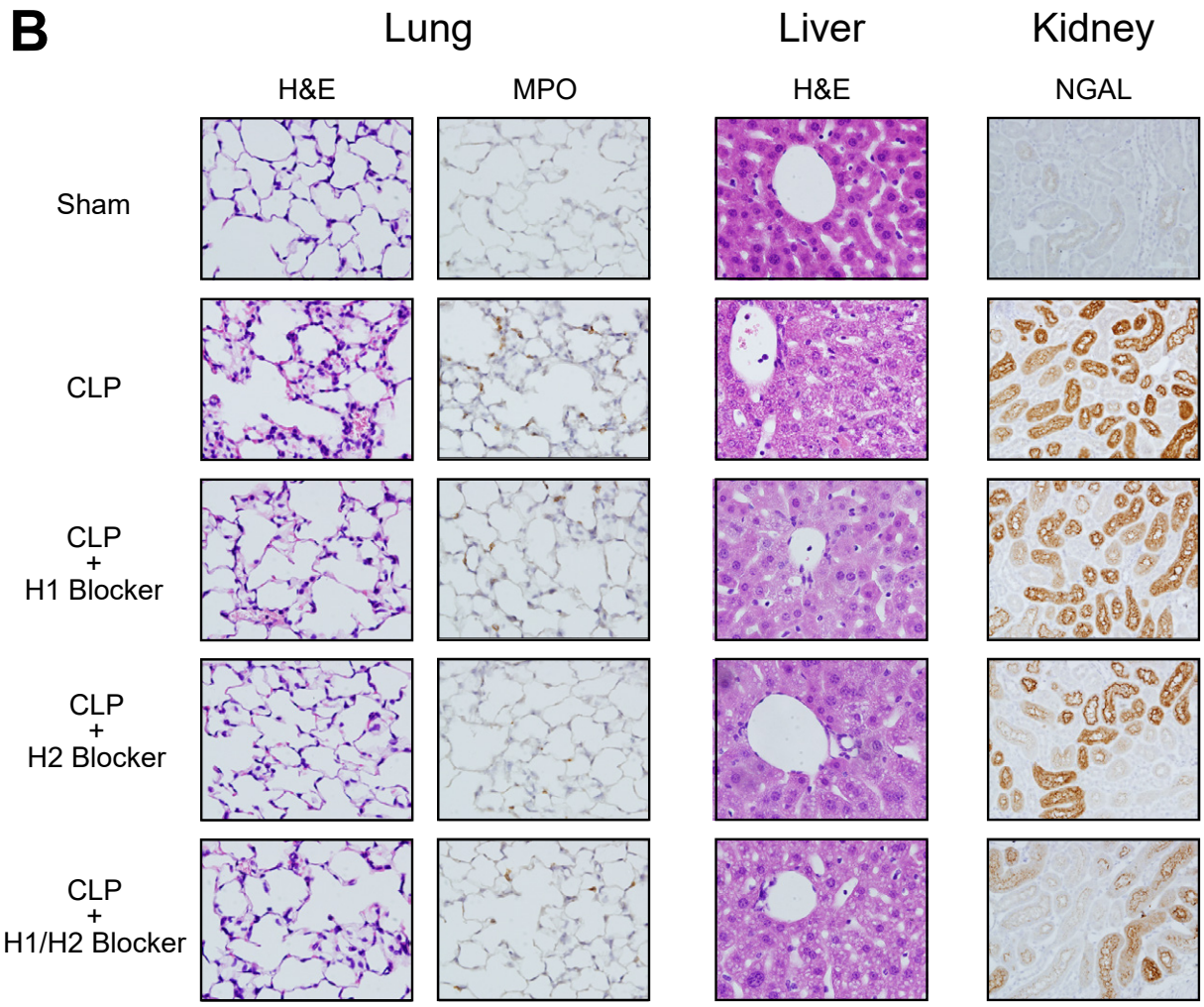
B
Lung
Liver
Kidney
H&E
MPO
H&E
NGAL
Sham
CLP
CLP + H1 Blocker
CLP + H2 Blocker
CLP + H1/H2 Blocker

Figure 7. Effects of treatment with *d*-chlorpheniramine and famotidine on elevated blood cytokines and organ injury following CLP-induced sepsis. Mice received intraperitoneal injection of *d*-chlorpheniramine (10 mg/kg) and famotidine (20 mg/kg), which were used as an H_1- and H_2-receptor blocker, respectively, at 60 min before CLP. *A*) Blood levels of IL-1β, IL-6, TNF-α, and MCP-1. The blood was collected 18 h after surgery (n = 3-19/group), and those cytokine levels were measured by the use of ELISA. All values are provided as means ± SEM. *P<0.05, **P<0.01, and ***P<0.001 *vs*. the respective control (18 h after sham operation). $^{\#}P$<0.05 and $^{\#\#}P$<0.01 *vs*. CLP alone. *B*) Representative micrographs tissue sections stained with hematoxylin and eosin, anti-MPO antibody, and anti-NGAL antibody. Lung, liver, and kidney tissues were harvested from sham-operated and CLP-induced septic mice 24 h after surgery. Original magnification, 200× (kidney) and 400× (lung, liver). The same results were obtained with two other experiments.

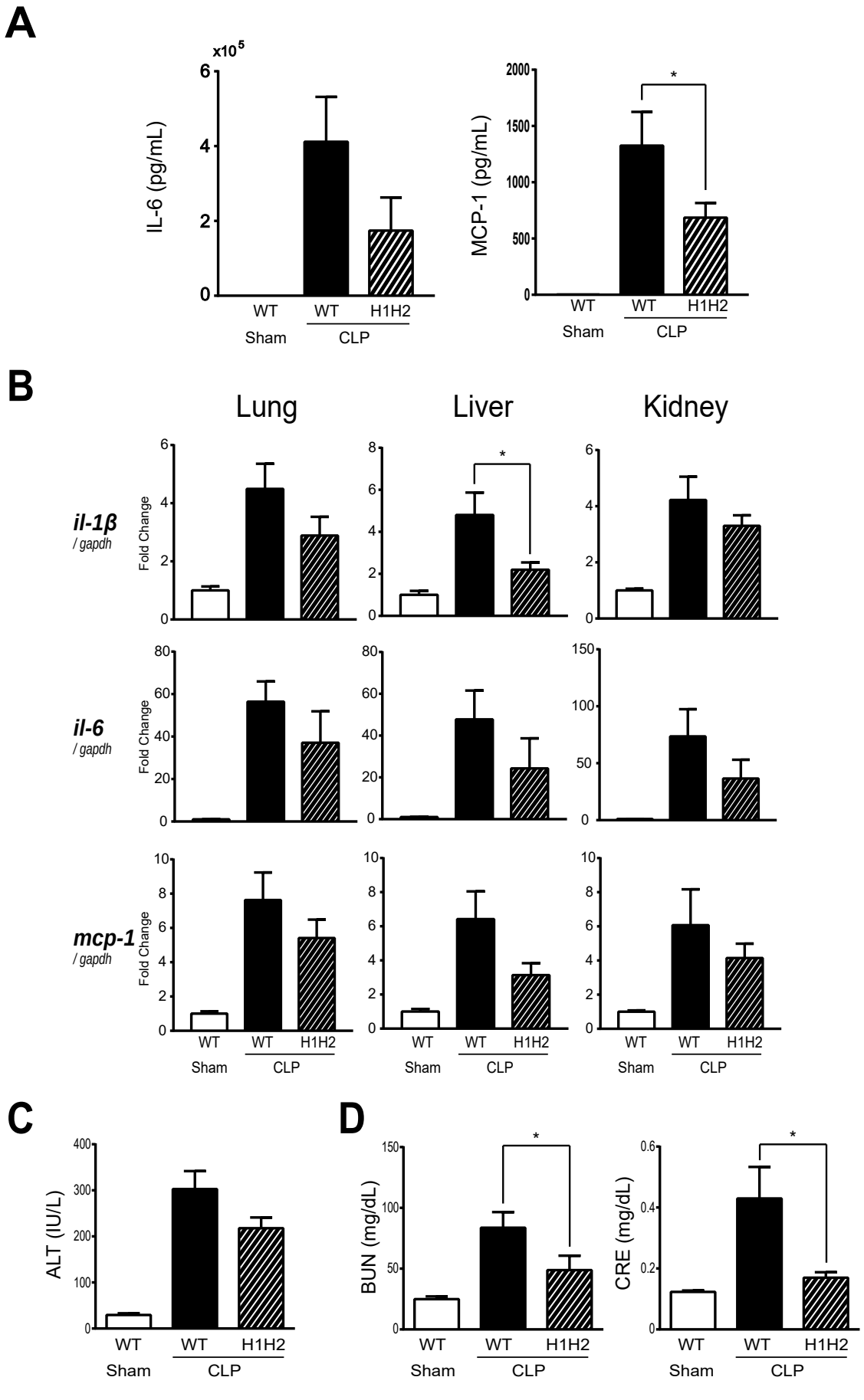
A
x10^5
IL-6 (pg/mL)
MCP-1 (pg/mL)
WT
WT
H1H2
Sham
CLP
B
Lung
Liver
Kidney
il-1β / gapdh
il-6 / gapdh
mcp-1 / gapdh
Fold Change
C
ALT (IU/L)
D
BUN (mg/dL)
CRE (mg/dL)

Figure 8. Cytokine levels and in liver and kidney functions in $H1R^{-/-}/H2R^{-/-}$ mice following CLP-induced sepsis. Blood and tissue samples were taken at 18 h after surgery (n = 5-8). *A*) Blood levels of IL-6 and MCP-1. *B*) Transcription levels of IL-1β, IL-6, and MCP-1 in lung, liver, and kidney tissues. *C*) Serum levels of ALT. *D*) Serum levels of BUN and creatinine. All values are provided as means ± SEM.

DISCUSSION

The specific pathophysiology and molecular basis of sepsis-associated multiple organ failure is still not fully understood. The updated definition of sepsis and septic shock has unveiled that organ dysfunction/failure is critical in determining the clinical outcome of sepsis (3). Here we provide clear evidence that histamine is identified as an aggravating mediator to contribute to the development of major end-organ (that is, lung, liver, and kidney) injury in sepsis.

Circulating levels of histamine were significantly elevated in mice after induction of polymicrobial sepsis by CLP, as fully demonstrated in our previous report (10). This elevation in the circulating histamine levels was associated with increased tissue expression of HDC, an enzyme that only forms histamine in mammals. This could result in locally elevated levels of histamine concentrations in tissues. Indeed, we found that histamine levels elevated in lung, liver, and kidney tissues in a time-dependent manner. In addition, the upregulation of gene expression levels of H_1- and H_2-receptors was observed after sepsis induction but quite varied between tissues. Taken together, these data shadow a possible role of histamine in the pathophysiology of sepsis.

Our CLP murine model of sepsis developed lung, liver, and kidney injury, as evidenced by histological changes, neutrophil filtration index, and biochemical variables. We found that sepsis-induced multiple organ injury was significantly attenuated in $HDC^{-/-}$ mice. This suggests that the lack of endogenous histamine could help to reduce sepsis-induced multiple organ injury. Alternatively, we interpret this finding to assume that histamine acts as a mediator to promote the development of multiple organ injury in sepsis. The attenuation of septic organ injury in $HDC^{-/-}$ mice may be partly the result of a reduction in cytokine production. Sepsis triggers overproduction of a diverse of proinflammatory

and chemotactic cytokines as demonstrated in this study. Their uncontrolled, exuberant production can be deleterious to various tissues and can lead to organ injury and dysfunction (24), although the pathogenesis of multiple organ dysfunction is multifactorial and is still being explored (25). In agreement with the present results on cytokines in $HDC^{-/-}$ mice, LPS-stimulated IL-6 production in liver tissues has been shown to fall to a low level in $HDC^{-/-}$ mice (26). Moreover, *in vitro* experiments have reported that histamine increases IL-6 production in B cells and glial cells (27), endothelial cells (28), and peripheral blood mononuclear cells (29), although there is found to be a report showing that histamine suppresses LPS-induced gene expression and synthesis of TNF-α in peripheral blood mononuclear cells mediated by H_2-receptors (30).

However, our experiments with the H_1-receptor antagonist *d*-chlorpheniramine and the H_2-receptor famotidine indicate that the lessening of sepsis-induced organ injury observed in $HDC^{-/-}$ mice cannot be solely attributed to alterations in proinflammatory and chemotactic cytokine production. These antagonists were not necessarily effective in reducing some cytokines in blood, such as IL-1β and IL-6, which is inconsistent with their changes obtained in $HDC^{-/-}$ mice. Yet, both *d*-chlorpheniramine and famotidine were effective in reducing septic lung and liver injury, whereas famotidine, but not *d*-chlorpheniramine, mitigated septic kidney injury. This suggests that, while both H_1- and H_2-receptors are involved in lung and liver injury, only H_2-receptors contribute to kidney injury in sepsis. The involvement of histamine via H_1-receptors in lung vascular hyperpermeability in sepsis has been documented (9, 31, 32). H_2-receptors have also been shown to be involved in the recruitment of neutrophils and protein leaks in LPS-induced acute lung injury (33). These adverse effects of histamine mediated by H_1- and H_2-receptors could be responsible for liver injury in sepsis. In renal ischemia/reperfusion injury, the beneficial effects of the H_2-receptor antagonist ranitidine have been found to be

partly mediated by decreased IL-6 production (34). Furthermore, it has been reported that mast cell-deficient mice exhibit attenuated acute kidney injury with cisplatin which is associated with reduced serum TNF-α levels and reduced recruitment of leukocytes to the inflamed kidney (35).

The transcription factor NF-κB has been well recognized as a pivotal player in the pathophysiology of sepsis (36). NF-κB is involved in regulating the transcription of many of the immunomodulatory mediators that can participate in the development of sepsis-induced organ failure (37). In a myriad of stimuli, commencing with endotoxin, IκBα is quickly phosphorylated, ubiquitinated, and degraded, releasing the NF-κB heterodimer, which then translocates from cytoplasm into nucleus to mediate the transcription of inflammatory genes (38). Interestingly, IκBα phosphorylation and degradation following CLP were impaired in lungs of $HDC^{-/-}$ mice. As a result, $HDC^{-/-}$ mice displayed low nuclear levels of NF-κB p65 in CLP-induced sepsis. We interpret these results to indicate that histamine can exert a facilitatory effect on activation of the NF-κB signaling pathway. Thus, histamine may help to promote the development of major end-organ injury in sepsis by enhancing NF-κB activity.

Contrary to the present findings indicative the role of H_2-receptor activation in worsening septic liver injury, a previous report has demonstrated that histamine pretreatment can ameliorate D-galactosamine/LPS-induced liver injury in WT and H_1-receptor knockout mice, but not H_2-receptor knockout mice (39). Furthermore, histamine through H_2-receptors has been documented to protect the liver against alcohol-induced injury in rats (40). It is difficult to reconcile these findings at present, but possible reasons for the discrepancy may include different regulatory mechanisms between systemic *vs*. local inflammation and concentration-related differences between endogenous *vs*. exogenous histamine.

It is now well established that histamine exerts its biological effects by binding to and activating four distinct separate receptors: H_1-, H_2-, H_3-, and H_4-receptors (41). Although our experiments with *d*-chlorpheniramine and famotidine imply that H_1- and H_2-receptors are involved in the development of septic organ injury, we cannot entirely exclude that the lack of activation of H_3- and H_4-receptors may contribute to reduced organ injury in $HDC^{-/-}$ mice following sepsis. Interestingly, H_4-receptors appear to play a role in sepsis-associated induction of apoptosis in the key organs (10). The exact role of H_3- and H_4-receptors in the pathophysiology of sepsis awaits further study using the animals deleted for their genes. It should be noted, however, that $H1R^{-/-}/H2R^{-/-}$ mice displayed lower blood biochemical values indicating the attenuation of sepsis-induced liver and renal dysfunction.

CONCLUSION

This study sheds light on the new role of histamine in the pathophysiology of sepsis. We represent the first report that endogenous histamine acting on H_1- and H_2-receptors leads to worsening of sepsis-driven major end-organ injury. Clinically, histamine H_2-receptor antagonists are widely used in critically ill patients to reduce the risk of gastrointestinal bleeding (42, 43). Histamine H_1-receptor antagonists may also be prescribed in perioperative settings, since many narcotics can induce itching (44). While our present study suggests the benefit of their treatment in reducing sepsis disorder and supports that they may be safe medications in critically ill patients with sepsis, the validity and feasibility of the use of these histamine receptor antagonists to avoid the development of septic organ injury warrant further clinical investigations and evaluation.

Acknowledgements

This research will never be materialized without the help of the following people and organizations:

First, I would like to express my gratitude and appreciation to Professor Mitsuaki Yamazaki (Department of Anesthesiology, Graduate School of Medicine and Pharmaceutical Sciences, University of Toyama), Professor Yuichi Hattori (Department of Molecular and Medical Pharmacology, Graduate School of Medicine and Pharmaceutical Sciences, University of Toyama) for their helpful guidance in my research work and preparing this dissertation, and for giving a chance of this research work.

I would like to thank Professor Johji Imura and Mr. Takeshi Nishida (Department of Diagnostic Pathology, Graduate School of Medicine and Pharmaceutical Sciences, University of Toyama), Professor Satoshi Tanaka (Department of Applied Mathematics, Faculty of Science, Okayama University of Science, Okayama), Professor Hiroshi Ohtsu (Department of Applied Quantum Medical Engineering, School of Engineering, Tohoku University, Sendai), Professor Naoyuki Matsuda (Department of Emergency and Critical Care Medicine, Nagoya University Graduate School of Medicine, Nagoya), Associate Professor Kenichiro Todoroki (Department of Analytical and Bio-Analytical Chemistry, School of Pharmaceutical Sciences, University of Shizuoka), Assistant Professor Wakana Ohashi (Department of Molecular and Medical Pharmacology, Graduate School of Medicine and Pharmaceutical Sciences, University of Toyama) for their excellent technical assistance, helpful guidance and valuable advice in my research work.

I would like to thank Dr. Mariko Takebe, Dr. Yuta Aoki, and Mr. Toshio Fujimori for their excellent technical assistance, helpful guidance and valuable advice in my research work.

Finally, I would like to express my gratitude to my family and members of the department (Department of Anesthesiology, Department of Molecular and Medical Pharmacology, Graduate School of Medicine and Pharmaceutical Sciences, University of Toyama) for their assistance in my life.

REFERENCES

1. Wang, H.E., Shapiro, N.I., Angus, D.C., and Yealy, D.M. (2007) National estimates of severe sepsis in Unites States emergency departments. *Crit. Care Med*. **35**, 1928-1936
2. Angus, D.C., and van der Poll, T. (2013) Severe sepsis and septic shock. *N. Engl. J. Med*. **369**, 840-851
3. Singer, M., Deutschman, C.S., Seymour, C.W., Shankar-Hari, M., Annane, D., Bauer, M., Bellomo, R., Bernard, G.R., Chiche, J.D., Coopersmith, C.M., Hotchkiss, R.S., Levy, M.M., Marshall, J.C., Martin, G.S., Opal, S.M., Rubenfeld, G.D., van der Poll, T., Vincent, J.L., Angus, D.C. (2016) The Third International Consensus Definitions for Sepsis and Septic Shock (Sepsis-3). *JAMA* **315**, 801-810
4. Gustot, T. (2011) Multiple organ failure in sepsis: prognosis and role of systemic inflammatory response. *Curr. Opin. Crit. Care* **17**, 153-159
5. Deutschman, C.S., and Tracey, K.J. (2014) Sepsis: current dogma and new perspectives. Immunity 40, 463-475
6. Rossaint, J., and Zarbock, A. (2015) Pathogenesis of multiple organ failure in sepsis. *Crit. Rev. Immunol*. **35**, 277-291
7. Matsuda, N., Hattori, Y., and Gando, S. (2004) Histamine and sepsis. In *Histamine: Biology and Medical Aspects* (Falus, A., Grosman, N., and Darvas, Zs, eds.), pp. 135-139, S. Karger AG, Basel
8. Matsuda, N., Hattori, Y., Sakuraya, F., Kobayashi, M., Zhang, X.H., Kemmotsu, O., and Gando, S. (2002) Hemodynamic significance of histamine synthesis and histamine H_1- and H_2-receptor gene expression during endotoxemia. *Naunyn-Schmiedeberg's Arch. Pharmacol*. **366**, 513-521
9. Matsuda, N., Hattori, Y., Takahashi, Y., Nishihira, J., Jesmin, S., Kobayashi, M., and Gando, S. (2004) Therapeutic effect of in vivo transfection of transcription factor decoy to NF-κB on septic lung in mice. *Am. J. Physiol. Lung Cell. Mol. Physiol*. **287**, L1248-L1255
10. Matsuda, N., Teramae, H., Futatsugi, M., Takano, K., Yamamoto, S., Tomita, K., Suzuki, T., Yokoo, H., Koike, K., and Hattori, Y. (2010) Up-regulation of histamine H_4 receptors contributes to splenic apoptosis in septic mice: Counteraction of antiapoptotic action of nuclear factor-κB. *J. Pharmacol. Exp. Ther*. **332**, 730-737
11. Matsuda, N., Hattori, Y., Zhang, X.H., Fukui, H., Kemmotsu, O., and Gando, S. (2003) Contractions to histamine in pulmonary and mesenteric arteries from endotoxemic rabbits: modulation by vascular expression of inducible nitric-oxide synthase and histamine H_1-receptors. *J. Pharmacol. Exp. Ther*. **307**, 175-181

12. Panula, P., Chazot, P.L., Cowart, M., Gutzmer, R., Leurs, R., Liu, W.L., Stark, H., Thurmond, R.L., and Haas, H.L. (2015) International Union of Basic and Clinical Pharmacology. XCVIII. Histamine Receptors. *Pharmacol. Rev*. **67**, 601-655
13. Hubbard, W.J., Choudhry, M., Schwacha, M.G., Kerby, J.D., Rue, L.W. 3rd, Bland, K.I., and Chaudry, I.H. (2005) Cecal ligation and puncture. *Shock* **24**, **Suppl 1**, 52-57
14. Ohtsu, H., Tanaka, S., Terui, T., Hori, Y., Makabe-Kobayashi, Y., Pejler, G., Tchougounova, E., Hellman, L., Gertsenstein, M., Hirasawa, N., Sakurai, E., Buzás, E., Kovács, P., Csaba, G., Kittel, A., Okada, M., Hara, M., Mar, L., Numayama-Tsuruta, K., Ishigaki-Suzuki, S, Ohuchi, K., Ichikawa, A., Falus, A., Watanabe, T., and Nagy, A. (2001) Mice lacking histidine decarboxylase exhibit abnormal mast cells. *FEBS Lett*. **502**, 53-56
15. Inoue, I., Yanai, K., Kitamura, D., Taniuchi, I., Kobayashi, T., Niimura, K., Watanabe, T., and Watanabe, T. (1996) Impaired locomotor activity and exploratory behavior in mice lacking histamine H_1 receptors. *Proc. Natl. Acad. Sci. U.S.A.* **93**, 13316-13320.
16. Kobayashi, T., Tonai, S., Ishihara, Y., Koga, R., Okabe, S., and Watanabe, T, (2000) Abnormal functional and morphological regulation of the gastric mucosa in histamine H2 receptor-deficient mice. *J. Clin. Invest*. **105**, 1741-1749.
17. Oishi, H., Takano, K., Tomita, K., Takeba, M., Yokoo, H., Yamazaki, M., and Hattori, Y. (2012) Olprinone and colforsin daropate alleviate septic lung inflammation and apoptosis through CREB-independent activation of the Akt pathway. *Am. J. Physiol. Lung Cell. Mol. Physiol*. **303**, L130-L140
18. Tomita, K., Takashina, M., Mizuno, N., Sakata, K., Hattori, K., Imura, J., Ohashi, W., and Hattori, Y. (2015) Cardiac fibroblasts: contributory role in septic cardiac dysfunction. *J. Surg. Res*. **193**, 874-887
19. Wang, Q., Yokoo, H., Takashina, M., Sakata, K., Ohashi, W., Abedelzaher, L.A., Imaizumi, T., Sakamoto, T., Hattori, K., Matsuda, N., and Hattori, Y. (2015) Anti-inflammatory profile of levosimendan in cecal ligation-induced septic mice and in lipopolysaccharide-stimulated macrophages. *Crit. Care Med*. **43**, e508-e520
20. Takano, K., Yamamoto, S., Tomita, K., Takashina, M., Yokoo, H., Matsuda, N., Takano, Y., Hattori, Y. (2011) Successful treatment of acute lung injury with pitavastatin in septic mice: Potential role of glucocorticoid receptor expression in alveolar macrophages. *J. Pharmacol. Exp. Ther*. 336, 381-390
21. Yamatodani, A., Fukuda, H., Wada, H., Iwaeda, T., and Watanabe, T. (1985) High-performance liquid chromatographic determination of plasma and brain histamine without previous purification of biological samples: cation-exchange chromatography coupled with pot-column derivatization fluorometry. *J. Chromatogr*. **344**, 115-123

22. Matsuda, N., Hattori, Y., Jesmin, S., Gando, S. (2005) Nuclear factor-κB decoy oligodeoxynucleotides prevent acute lung injury in mice with cecal ligation and puncture-induced sepsis. *Mol. Pharmacol*. **67**, 1018-1025.
23. Takebe, M., Oishi, H., Taguchi, K., Aoki, Y., Takashina, M., Tomita, K., Yokoo, H., Takano, Y., Yamazaki, M., Hattori, Y. (2014) Inhibition of histone deacetylases protects septic mice from lung and splenic apoptosis. *J. Surg. Res*. **187**, 559-570
24. Benjamin, C.F., Hagaboam, C.M., Kunkel, S.L. (2004) The chronic consequences of severe sepsis. *J. Leukoc. Biol*. **75**, 408-412
25. Wang, H., Ma, S. (2008) The cytokine storm and factors determining the sequence and severity of organ dysfunction in multiple organ dysfunction syndrome. *Am. J. Emerg. Med*. **26**, 711-715
26. Horváth, B.V., Falus, A., Tóth, S., Szalai, Cs., Lázár-Molnár, E., Holub, M.Cs., Buzás, E., Nagy, A., Fulop, A.K. (2002) Inverse regulation of interleukin-6 (IL-6) and IL-6 receptor in histamine deficient histidine decarboxylase-knock-out mice. *Immunol. Lett*. **80**, 151-154
27. Falus, A. (1993) Interleukin-6 biosynthesis is increased by histamine in human B-cell and glioblastoma cell lines. *Immunology* **78**, 193-196
28. Delneste, Y., Lassalle, P., Jeannin, P., Joseph, M., Tonnel, A.B., Gosset, P. (1994) Histamine induces IL-6 production by human endothelial cells. *Clin. Exp. Immunol*. **98**, 344-349
29. Mor, S., Nagler, A., Barak, V., Handzel, Z.T., Geller-Bernstein, C., Fabian, I. (1995) Histamine enhances granulocyte-macrophage colony-stimulating factor and interleukin-6 by human peripheral blood mononuclear cells. *J. Leukoc. Biol*. **58**, 445-450
30. Vannier, E., Miller, L.C., Dinarello, C.A. (1991) Histamine suppresses gene expression and synthesis of tumor necrosis factor α via histamine H_2 receptors. *J. Exp. Med*. **174**, 281-284
31. Brigham, K.L., Padove, S.J., Bryant, D., McKeen, C.R., Bowers, R.E. (1980) Diphenhydramine reduces endotoxin effects on lung vascular permeability in sheep. *J. Appl. Physiol*. **49**, 516-520
32. Sielaff, T.D., Sugerman, H.J., Tatum, J.L., Kellum, J.M., Blocher, C.R. (1987) Treatment of porcine *Pseudomonas* ARDS with combination drug therapy. *J. Trauma* 27, 1313-1322
33. Kim, T.H., Yoon, H.J., Lim, C.M., Kim, E.K., Kim, M.J., Koh, Y. (2005) The role of endogenous histamine on the pathogenesis of the lipopolysaccharide (LPS)-induced, acute lung injury: a pilot study. *Inflammation* **29**, 72-80

34. Vannay, A., Fekete, A. Müller, V., Strehlau, J., Viklicky, O., Veres, T., Reusz, G., Tulassay, T., Szabó, A.J. (2004) Effects of histamine and the h2 receptor antagonist ranitidine on ischemia-reperfusion acute renal failure: involvement of IL-6 and vascular endothelial growth factor. *Kidney Blood Press. Res*. **27**, 105-113
35. Summers, S.A., Chan, J., Gan, P.Y., Dewage, L., Nozaki, Y., Steinmetz, O.M., Nikolic-Paterson, D.J., Kitching, A.R., Holdsworth, S.R. (2011) Mast cells mediate acute kidney injury through the production of TNF. *J. Am. Soc. Nephrol*. **22**, 2226-2236
36. Liu, S.F., Malik, A.B. (2006) NF-κB activation as a pathological mechanism of septic shock and inflammation. *Am. J. Physiol. Lung Cell. Mol. Physiol*. **290**, L622-L645
37. Abraham, E. (2003) Nuclear factor-kappaB and its role in sepsis-associated organ failure. *J. Infect. Dis*. **187 (Suppl 2)**, S364-S369
38. Ghosh, S., May, M.J., Kopp, E.B. (1998) NF-kappa B and Rel proteins: Evolutionarily conserved mediators of immune responses. *Annu. Rev. Immunol*. **16**, 225-260
39. Masaki, T., Chiba, S., Tatsukawa, H., Noguchi, H., Kakuma, T., Endo, M., Seike, M., Watanabe, T., Yoshimatsu, H. (2005) The role of histamine H_1 receptor and H_2 receptor in LPS-induced liver injury. *FASEB J*. **19**, 1245-1252
40. Hornyak, S.C., Gehlsen, K.R., Haaparanta, T. (2003) Histamine dihydrochloride protects against early alcohol-induced liver injury in a rat model. *Inflammation* 27, 317-327
41. Panula, P., Chazot, P.L., Cowart, M., Gutzmer, R., Leurs, R., Liu, W.L., Stark, H., Thurmond, R.L., Haas, H.L. (2015) International Union of Basic and Clinical Pharmacology. XCVIII. Histamine Receptors. *Pharmacol. Rev*. **67**, 601-655
42. Brett, S. (2005) Science review: The use of proton pump inhibitors for gastric acid suppression in critical illness. *Crit. Care* **9**, 45-50
43. Herzig, S.J., Howell, M.D., Ngo, L.H., Marcantonio, E.R. (2009) Acid-suppressive medication use and the risk for hospital-acquired pneumonia. *JAMA* **301**, 2120-2128
44. St. Peter S.D., Sharp, S.W., Ostlie, D.J. (2010) Influence of histamine receptor antagonists on the outcome of perforated appendicitis: analysis from a prospective trial. *Arch. Surg*. **145**, 143-146.